



# A simple approach for the computation of Lyapunov–Floquet transformations for general time-periodic systems

Ashu Sharma<sup>1</sup>

Received: 7 January 2024 / Revised: 31 March 2024 / Accepted: 18 April 2024  
© The Author(s), under exclusive licence to Springer-Verlag GmbH Germany, part of Springer Nature 2024

## Abstract

Ordinary differential equations with time-periodic coefficients (so-called time-periodic systems) can be analyzed using Lyapunov–Floquet (L–F) transformations. These transformations reduce the linear part of a time-periodic equation to the time-invariant form and facilitate the application of well-established techniques tailored for time-invariant systems. In the previous work, the construction of L–F transformations relied on Chebyshev polynomials and their properties, which may often prove challenging to grasp and apply effectively. This paper endeavors to present a more intuitive and straightforward approach for computing L–F transformations. The solution of a linear time-periodic system can be expressed as a product of an exponential function and a vector-valued polynomial in time with time-periodic coefficients. Substitution of the solution reduces a time-periodic equation to an eigenvalue problem, which can be solved to obtain the general solution. Rearranging the solution yields the state transition matrix, which can be used in the Lyapunov–Floquet theorem to compute the L–F transformation. The inverse of these transformations is important for the nonlinear analysis and control and can be determined by defining the adjoint system to the time-periodic system. As examples, L–F transformations and their inverses are generated for the Mathieu equation and a double inverted pendulum subjected to a time-periodic force. In the end, the usefulness of L–F transformations is showcased by performing the bifurcation study of a nonlinear Mathieu equation using the center manifold theorem.

**Keywords** Time-periodic systems · Floquet theory · Lyapunov–Floquet theorem · Lyapunov–Floquet transformation · Mathieu equation

## 1 Introduction

Ordinary differential equations with time-periodic coefficients (so-called time-periodic systems) are used to model numerous physical systems in various fields of science and engineering. The study of these systems dates back to 1868 when Mathieu [1] analyzed the vibration of an elliptic membrane.

Shortly afterward, in 1883, M.G. Floquet developed a complete mathematical theory (commonly known as Floquet theory [2, 3]) to determine the stability and response of linear time-periodic systems. Since then, several numerical [4],

analytical [5, 6], and symbolic [7, 8] techniques have been developed to compute the stability and response of time-periodic systems using the Floquet theory. Time-periodic systems can also be investigated using the Lyapunov–Floquet (L–F) theorem [9], which allows the transformation of such systems to a system of equations whose linear parts are time-invariant. L–F transformations can be useful for studying time-periodic systems as many existing techniques applicable to time-invariant systems can be used for such problems. For instance, bifurcation studies require nonlinear equations of perturbed dynamics. If the linear part of the equations can be made time-invariant via L–F transformation, the resulting nonlinear equations can be simplified using local nonlinear techniques such as time-dependent normal form theory and center manifold reduction [10, 11]. Furthermore, controllers can be designed using time-invariant methods [12, 13]. In ref. [14], it is shown that analysis of time-periodic systems using L–F transformations is free from limitations such as

---

A small part of this work was presented at the IDETC/CIE 2021 virtual conference, August 17–19, 2021.

---

✉ Ashu Sharma  
ashusharma.dtu@gmail.com

<sup>1</sup> Department of Mechanical Engineering, Auburn University, Auburn, AL 36849, USA

the existence of a small parameter and a generating solution, restrictions owned by classical techniques (method of averaging and perturbation techniques).

L–F transformations can be computed in closed forms for a special class of time-periodic systems, called the commutative systems [15]. Such a transformation can be constructed for a general time-periodic system if the state transition matrix (STM) is known as an explicit function of time. In 1991, Sinha and Wu [16] developed an efficient technique for the computation of the STM of a general time-periodic system using shifted Chebyshev polynomials of the first kind. Using this work in 1996, Sinha et al. [17] presented a technique for the computation of L–F transformations for general time-periodic systems. In 2009, Butcher et al. [18] proposed a technique to determine L–F transformation in a symbolic form using Magnus expansion. Their approach seems to work for general periodic systems and does not require the computation of STM in a symbolic form. However, it does not yield good results even for the Mathieu equation with relatively smaller values of system parameters [8]. In 2016, Kirkland and Sinha [8] first implemented Chebyshev expansion and Picard iteration methods as suggested in ref. [7] to compute the STM symbolically and then utilized a Gaussian quadrature integral formula and matrix exponential summation method to determine L–F transformation in symbolic form. Unlike ref. [18], their approach seems to work for a wide range of system parameters.

While the L–F transformations-based approach offers distinct advantages over classical techniques, its broader adoption within the scientific community has been limited, perhaps due to the intricacies associated with the incorporation of Chebyshev polynomials in constructing these transformations. Recognizing this challenge, the present paper introduces a novel, intuitive, and simplified methodology for computing L–F transformations, aiming to enhance accessibility and encourage wider application of this valuable technique in scientific research and engineering domains. The proposed approach differs from the previous methods [8, 17] in determining the STM of a time-periodic system. First, an assumed form of solution (Floquet form) is utilized to reduce a linear time-periodic equation to an eigenvalue problem, which is then solved to compute the general solution and construct the STM. Once the STM is known, L–F transformation is obtained using the L–F theorem. It is worth noting that the Floquet form, initially used by Hill to determine lunar perigee [19], has been widely used to compute the stability of linear time-periodic systems. The present work's contribution lies in demonstrating that, using the Floquet form, the L–F transformations can be very easily generated for general time-periodic systems. To the author's best knowledge, no one has attempted to use this type of approach to construct L–F transformations, even for the trivial (stable and unstable) cases of the Mathieu equation. This paper uses the proposed

method and computes L–F transformations and their inverses for not only stable and unstable cases but also the critical case of one and two degrees-of-freedom systems. Critical cases are particularly important compared to trivial cases, as nonlinearities play an imperative role in describing the behavior of systems. A bifurcation study is also presented to demonstrate the effectiveness of L–F transformation.

The approach proposed in this paper is more intuitive and straightforward because it is developed along the lines of time-invariant systems where the general solution is determined by substituting an assumed solution in the differential equation and then performing the eigenanalysis to calculate eigenvalues and eigenvectors.

## 2 Mathematical background

A set of nonlinear ordinary differential equations with time-periodic coefficients is given by

$$\dot{\mathbf{x}} = \mathbf{A}(t)\mathbf{x} + \mathbf{w}_2(\mathbf{x}, t) + \dots + \mathbf{w}_\chi(\mathbf{x}, t) + \mathbf{O}\left(|\mathbf{x}|^{\chi+1}, t\right), \quad (1)$$

where  $\mathbf{x} \in \mathbb{R}^{n \times 1}$ ,  $\mathbf{A}(t)$  is a  $n \times n$  time-periodic matrix function with the principal period  $T$ ,  $\mathbf{w}_\chi(\mathbf{x}, t)$  are  $n \times 1$  nonlinear vectors containing homogenous monomials in  $\mathbf{x}$  (of order  $\chi$ ) with time-periodic coefficients and  $t$  is the time. Equation (1) can be rewritten in the compact form as

$$\dot{\mathbf{x}} = \mathbf{A}(t)\mathbf{x} + \mathbf{W}(\mathbf{x}, t), \quad (2)$$

where  $\mathbf{W}(\bullet)$  is appropriately defined in terms of  $\mathbf{w}_\chi(\bullet)$ . The linear homogenous part of Eq. (2) is given by

$$\dot{\mathbf{x}} = \mathbf{A}(t)\mathbf{x}, \quad (3)$$

whose stability and response can be determined using the well-known Floquet theory [2, 3]. Let  $\Phi(t)$  be the STM such that it satisfies Eq. (3) with  $\Phi(0) = \mathbf{I}$ ; then, the solution of Eq. (3) is given by

$$\mathbf{x}(t) = \Phi(t)\mathbf{x}(0) \quad ; \quad 0 \leq t \leq T. \quad (4)$$

According to the Lyapunov–Floquet theorem [9], the STM can be factored as

$$\Phi(t) = \mathbf{L}(t)\mathbf{e}^{\mathbf{C}t}; \quad \mathbf{L}(t) \in \mathbb{C}^{n \times n}; \quad \mathbf{C} \in \mathbb{C}^{n \times n} \quad \forall t \geq 0, \quad (5)$$

or,

$$\Phi(t) = \mathbf{Q}(t)\mathbf{e}^{\mathbf{R}t}; \quad \mathbf{Q}(t) \in \mathbb{R}^{n \times n}, \quad \mathbf{R} \in \mathbb{R}^{n \times n} \quad \forall t \geq 0, \quad (6)$$

where  $\mathbf{L}(t)$  and  $\mathbf{Q}(t)$  are  $T$  periodic and  $2T$  periodic L–F transformations, respectively. Using the transformation,

$\mathbf{x} = \mathbf{L}(t)\mathbf{z}$  or  $\mathbf{x} = \mathbf{Q}(t)\mathbf{z}$ , Eq. (3) can be reduced to

$$\dot{\mathbf{z}} = \mathbf{C}\mathbf{z} \quad \text{or} \quad \dot{\mathbf{z}} = \mathbf{R}\mathbf{z}, \quad \text{respectively,} \quad (7)$$

where  $\mathbf{C}$  and  $\mathbf{R}$  are time-invariant matrices and are defined as

$$\mathbf{C} = \frac{1}{T} \ln \Phi(T) \quad \text{and} \quad \mathbf{R} = \frac{1}{2T} \ln \Phi(2T). \quad (8)$$

Here,  $\Phi(T)$  is the Floquet transition matrix (FTM) or the monodromy matrix.

The stability of linear time-periodic systems depends upon the eigenvalues of  $\Phi(T)$ , commonly known as ‘Floquet multipliers’. In general, the Floquet multipliers,  $\rho_j$ ;  $j = 1, \dots, n$  are complex and the system is stable if  $|\rho_j| \leq 1$ , i.e., all Floquet multipliers lie on or inside the unit circle, otherwise it is unstable. In the case of  $|\rho_j| = 1$ ,  $\rho_j$  should be a simple root of the FTM for the stability of the system. The stability of linear time-periodic systems can also be defined in terms of ‘characteristic exponents’ (eigenvalues of the time-invariant matrix  $\mathbf{C}$ ). The characteristic exponents,  $\lambda_j = \alpha_j + i\beta_j$  are defined as

$$\alpha_j = \frac{1}{T} \ln |\rho_j| \quad \text{and} \quad \beta_j = \frac{1}{T} (\arg \rho_j + 2\bar{N}\pi); \quad \bar{N} \in \mathbb{Z}. \quad (9)$$

The system is stable if all  $\alpha_j \leq 0$ , otherwise it is unstable. In the case of zero or purely imaginary characteristic exponents, the time-periodic system is stable if  $\lambda_j$  is a simple root of the time-invariant matrix  $\mathbf{C}$ . It should be noted that characteristic exponents are not unique and any  $\lambda_j$  can be replaced by  $\lambda_j + 2\bar{N}\pi i/T$ .

Application of the transformation,  $\mathbf{x} = \mathbf{L}(t)\mathbf{z}$  or  $\mathbf{x} = \mathbf{Q}(t)\mathbf{z}$  to Eq. (2) yields

$$\dot{\mathbf{z}} = \mathbf{C}\mathbf{z} + \mathbf{L}^{-1}(t)\mathbf{W}(\mathbf{L}(t)\mathbf{z}, t) \quad \text{or} \quad \dot{\mathbf{z}} = \mathbf{R}\mathbf{z} + \mathbf{Q}^{-1}(t)\mathbf{W}(\mathbf{Q}(t)\mathbf{z}, t). \quad (10)$$

It is evident that Eq. (2) can be analyzed using Eq. (10); however, the investigation requires the computation of L–F transformation and its inverse.

**Remark** If one of the Floquet multipliers lies in the left half of the complex plane, then, the real L–F transformation,  $\mathbf{Q}(t)$ , is  $2T$  periodic and has symmetry of  $\mathbf{Q}(t + T) = -\mathbf{Q}(t)$ . However, if all the Floquet multipliers lie in the right half of the complex plane, the real and complex transformations coincide, both being  $T$  periodic and real.

### 3 Computation of Lyapunov–Floquet transformations

The solution of Eq. (3) has the form [3]

$$\mathbf{x} = e^{\lambda t} \mathbf{p}^1(t), \quad (11)$$

where  $\lambda$  is the characteristic exponent, and  $\mathbf{p}^1(t) = \{p^{11}(t), p^{12}(t), \dots, p^{1n}(t)\}^T$  is a periodic vector function with period  $T$ . If  $p^{1r}(t) = \sum_{s=-N}^{s=+N} c_s^{1r} e^{is\omega t}$ ;  $r = 1, 2, \dots, n$ , substituting Eq. (11) in Eq. (3) and then equating the coefficients of  $e^{is\omega t}$  leads to

$$\mathbf{K}(\lambda) \mathbf{c}^1 = \mathbf{0}; \quad \mathbf{c}^1 = \{c_{-N}^{11}, \dots, c_N^{11}, \dots, c_{-N}^{1n}, \dots, c_N^{1n}\}^T, \quad (12)$$

where  $\mathbf{K}(\lambda)$  is a  $n(2N + 1) \times n(2N + 1)$  and is commonly known as Hill matrix. Equation (12) is an eigenvalue problem where  $\lambda$  is the eigenvalue and  $\mathbf{c}^1$  is the eigenvector. For the non-trivial solution of  $\mathbf{c}^1$ , the determinant of  $\mathbf{K}(\lambda)$  can be set to zero to determine  $n(2N + 1)\lambda's$ . Equation (3) is an  $n^{th}$  order system, and therefore, the number of  $\lambda's$  should be equal to  $n$  and they can be obtained by using the constraint  $-\pi/T < \text{Im}[\lambda_j] \leq \pi/T$ . The rest of the  $\lambda's$  are dependent on these  $n \lambda's$  (see the non-uniqueness property of exponents in Sect. 2). If  $\lambda_1$  through  $\lambda_n$  satisfies the constraint, they can be used to plot stability chart. Also, corresponding eigenvectors can be determined using Eq. (12) to construct the general solution of Eq. (3) as

$$\mathbf{x}(t) = A_1 \mathbf{x}_1(t) + A_2 \mathbf{x}_2(t) + \dots + A_n \mathbf{x}_n(t), \quad (13)$$

where  $\mathbf{x}_j(t)$ ;  $j = 1, \dots, n$  are the  $n$  linearly independent solutions, and they have the form of Eq. (11) only when eigenvalues  $\lambda_1$  through  $\lambda_n$  are distinct. Using the initial condition, scalar constants  $A_1$  through  $A_n$  can be determined, and then, Eq. (13) can be rearranged in the form of Eq. (4) to yield  $\Phi(t)$  for Eq. (3).

If eigenvalues  $\lambda_j's$  that satisfy the constraint are not distinct, all linearly independent solutions of Eq. (3) cannot have the form of Eq. (11). Suppose the eigenvalue  $\lambda_j$  of Eq. (3) has algebraic multiplicity  $\Gamma$  and geometric multiplicity  $\Lambda$ . Then, there are  $\Lambda (< \Gamma)$  linearly independent solutions of Eq. (3), and each solution has the form of Eq. (11). To get the rest  $(\Gamma - \Lambda)$  linearly independent solutions, the following form solution must be assumed.

$$\mathbf{x} = e^{\lambda t} \left[ t \mathbf{p}^1(t) + \mathbf{p}^2(t) \right], \quad (14)$$

where  $\mathbf{p}^2(t) = \{p^{21}(t), p^{22}(t), \dots, p^{2n}(t)\}^T$  is a periodic vector function with period  $T$  and  $p^{2r}(t) = \sum_{s=-N}^{s=+N} c_s^{2r} e^{is\omega t}$ .

Substituting Eq. (14) in Eq. (3) and then equating the coefficients of  $e^{is\omega t}$  yields

$$\mathbf{K}(\lambda)\mathbf{c}^1 = \mathbf{0}, \tag{15a}$$

$$\mathbf{K}(\lambda)\mathbf{c}^2 = \mathbf{c}^1; \mathbf{c}^2 = \left\{ c_{-N}^{21}, \dots, c_N^{21}, \dots, c_{-N}^{2n}, \dots, c_N^{2n} \right\}^T. \tag{15b}$$

Equation (15a) and Eq. (12) are the same and the eigenvector  $\mathbf{c}^1$  obtained from Eq. (12) can be substituted in Eq. (15b) to determine the generalized eigenvector  $\mathbf{c}^2$ . If there are  $\Upsilon$  linearly independent generalized eigenvectors  $\mathbf{c}^2$ , then, there are an additional  $\Upsilon$  linearly independent solutions of Eq. (3) of the form of Eq. (14). In the case  $\Lambda + \Upsilon = \Gamma$ , there is no need to proceed further as there is a full quota of solutions corresponding to eigenvalue  $\lambda_j$ . However, if  $\Lambda + \Upsilon < \Gamma$ , the following form of the solution must be assumed to increase the number of independent solutions from  $(\Lambda + \Upsilon)$  to  $\Gamma$ .

$$\mathbf{x} = e^{\lambda t} \left[ \frac{t^2}{2} \mathbf{p}^1(t) + t \mathbf{p}^2(t) + \mathbf{p}^3(t) \right], \tag{16}$$

where  $\mathbf{p}^3(t) = \{ p^{31}(t), p^{32}(t), \dots, p^{3n}(t) \}^T$  with  $p^{3r}(t) = \sum_{s=-N}^{s=+N} c_s^{3r} e^{is\omega t}$ . Substitution into Eq. (3) and then equating the coefficients of  $e^{is\omega t}$  leads to the following three equations.

$$\mathbf{K}(\lambda)\mathbf{c}^1 = \mathbf{0}, \tag{17a}$$

$$\mathbf{K}(\lambda)\mathbf{c}^2 = \mathbf{c}^1, \tag{17b}$$

$$\mathbf{K}(\lambda)\mathbf{c}^3 = \mathbf{c}^2; \mathbf{c}^3 = \left\{ c_{-N}^{31}, \dots, c_N^{31}, \dots, c_{-N}^{3n}, \dots, c_N^{3n} \right\}^T. \tag{17c}$$

Equations (17a) and (17b) have been solved previously, and they can be used to compute generalized eigenvector  $\mathbf{c}^3$ . More independent solutions are obtained, and this process is continued until  $\Gamma$  independent solutions corresponding to the eigenvalue  $\lambda_j$  are generated. After determining solutions corresponding to all eigenvalues,  $\Phi(t)$  can be constructed and then can be substituted in Eq. (8) to get a time-invariant matrix  $\mathbf{C}$  (or  $\mathbf{R}$ ) and subsequently, L–F transformations  $\mathbf{L}(t)$  (or  $\mathbf{Q}(t)$ ) can be computed using Eq. (5) (or 6).

From Eq. (10), it can be seen that the analysis of time-periodic systems using L–F transformations require the computation of their inverse. It can be computed by defining the adjoint system to Eq. (3) as

$$\dot{\mathbf{x}} = -\mathbf{A}^T(t)\mathbf{x}. \tag{18}$$

If  $\Psi(t)$  is the STM of Eq. (18), which can be computed using the process described above, according to ref. [9], the

following relationship holds.

$$\Phi^{-1}(t) = \Psi^T(t). \tag{19}$$

Using Eqs. (5) and (6),  $\mathbf{L}^{-1}(t)$  and  $\mathbf{Q}^{-1}(t)$  can be written as

$$\mathbf{L}^{-1}(t) = \mathbf{e}^{\mathbf{C}t} \Phi^{-1}(t) = \mathbf{e}^{\mathbf{C}t} \Psi^T(t), \tag{20}$$

$$\mathbf{Q}^{-1}(t) = \mathbf{e}^{\mathbf{R}t} \Phi^{-1}(t) = \mathbf{e}^{\mathbf{R}t} \Psi^T(t). \tag{21}$$

### 4 Examples

Two time-periodic systems are examined in this paper. Mathieu equation representing one degree-of-freedom systems is considered as a first example, whereas the second example involves a higher order system: a double inverted pendulum subjected to a time-periodic force. In both examples, the stability diagrams are first constructed to identify the system parameters for stable, unstable and critical cases. Then, L–F transformations and their inverses are generated for stable, unstable and critical cases of the Mathieu equation and the critical case of the double inverted pendulum. The second example is investigated to show that the proposed approach can be easily applied to higher order systems.

#### 4.1 Mathieu equation

A damped Mathieu equation can be written in the state space form as

$$\dot{\mathbf{x}} = \begin{bmatrix} 0 & 1 \\ -(a + b \cos \omega t) & -d \end{bmatrix} \mathbf{x}; \mathbf{x}(0) = \begin{bmatrix} x_0 \\ \dot{x}_0 \end{bmatrix}, \tag{22}$$

where  $\{a, b, d\}$  are the system parameters,  $\omega$  is the parametric excitation frequency and the coefficient matrix  $\mathbf{A}(t)$  is periodic with principal period  $T = 2\pi / \omega$ .

Substituting Eq. (11) with  $n = 2$  in Eq. (22) and equating the coefficients of  $e^{is\omega t}$  leads to

$$c_s^{11}(\lambda + is\omega) = c_s^{12}, \tag{23a}$$

$$c_s^{12}(\lambda + is\omega) = -ac_s^{11} - dc_s^{12} - (b/2)(c_{s-1}^{11} + c_{s+1}^{11}), \tag{23b}$$

which can be rearranged in the form of Eq. (12). Substituting  $c_s^{12}$  from Eq. (23a) in Eq. (23b) halves the total number of equations. Equation (23b) takes the form

$$\left[ (\lambda + is\omega)^2 + d(\lambda + is\omega) + a \right] c_s^{11} + (b/2)(c_{s-1}^{11} + c_{s+1}^{11}) = 0, \tag{24}$$

and can be rewritten in the matrix form as

$$\overline{\mathbf{K}} \overline{\mathbf{c}}^1 = \begin{bmatrix} k_{-N} & \frac{b}{2} & & & & \\ & \frac{b}{2} & \ddots & & & \\ & & \ddots & \frac{b}{2} & & \\ & & & k_0 & \ddots & \\ & & & & \ddots & \frac{b}{2} \\ & & & & & \frac{b}{2} & k_N \end{bmatrix} \begin{bmatrix} c_{-N}^{11} \\ \vdots \\ c_0^{11} \\ \vdots \\ c_N^{11} \end{bmatrix} = \begin{bmatrix} 0 \\ \vdots \\ 0 \\ \vdots \\ 0 \end{bmatrix}, \quad (25)$$

where  $k_s = [(\lambda + is\omega)^2 + d(\lambda + is\omega) + a]$  and  $s$  varies from  $-N$  to  $N$ . Equation (25) is a quadratic eigenvalue problem where  $\lambda$  is the eigenvalue and  $\overline{\mathbf{c}}^1$  is the eigenvector.

It is well-known that at stability boundaries, the solution of one degree-of-freedom time-periodic system is either  $T$  periodic or  $2T$  periodic with  $0$  and  $i\pi/T$ , respectively, as one of the exponents. Substitution of these values in  $\text{Det}[\overline{\mathbf{K}}] = 0$  yields polynomial expressions for both  $T$  and  $2T$  periodic boundaries in terms of system parameters  $\{a, b, d\}$  and parametric excitation frequency,  $\omega$ . Using  $\omega = 1$  and  $d = 0$  in these expressions, the stability diagram of Eq. (22) is plotted in the  $a \sim b$  plane defined by  $-1 \leq a \leq 10$  and  $0 \leq b \leq 10$  and is shown in Fig. 1. It is found that the stability diagram obtained using  $N = 10$  in  $\text{Det}[\overline{\mathbf{K}}] = 0$  is in excellent agreement with the numerically obtained stability diagram.

Stable and unstable regions are clearly visible in Fig. 1. System parameters for stability and instability are identified and shown in Table 1. For the critical case, system parameters are determined using polynomial expressions for stability boundaries and are also tabulated in Table 1.

### 4.1.1 L–F transformations and their inverses for stable and unstable cases

The Mathieu equation is stable for  $a = 4$  and  $b = 4$ . Setting  $\text{Det}[\overline{\mathbf{K}}] = 0$  and using the constraint  $-0.5 < \text{Im}[\lambda_j] \leq +0.5$ , eigenvalues are determined and are tabulated in col. 4 of Table 1. All the eigenvalues are distinct, and thus, all the independent solutions are of the form of Eq. (11). Eigenvectors corresponding to these  $\lambda_j$ s can be determined with the help of Eq. (25). In the case of distinct eigenvalues, eigenvectors are related. If the eigenvector corresponding to the complex eigenvalue  $\lambda_1 = \lambda$  is

$$\overline{\mathbf{c}}^1 = \{ c_{-10}^{11} \dots c_0^{11} \dots c_{10}^{11} \}^T, \quad (26)$$

then, the eigenvector corresponding to the complex conjugate  $\lambda_2 = \overline{\lambda}$  is

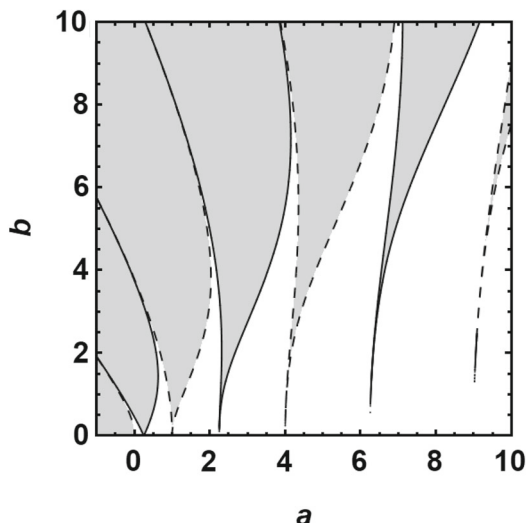


Fig. 1 Stability diagram of the Mathieu equation (Eq. (22)). Gray: numerically computed unstable regions, black solid:  $2T$  boundaries using the proposed method, black dashes:  $T$  periodic boundaries using the proposed method

$$\overline{\mathbf{c}}^1 = \{ c_{10}^{11} \dots c_0^{11} \dots c_{-10}^{11} \}^T. \quad (27)$$

The case of distinct real eigenvalues is not very different from the case of distinct complex eigenvalues because if  $\lambda_1 = a_1 - \sqrt{b_1}$  and  $\lambda_2 = a_1 + \sqrt{b_1}$  are the distinct real eigenvalues, they can be rewritten as  $\lambda_1 = a_1 + i\overline{b_1}$  and  $\lambda_2 = a_1 - i\overline{b_1}$  with  $\overline{b_1} = i\sqrt{b_1}$ . These relationships between eigenvectors are valid for general time-periodic systems.

Once eigenvalues and eigenvectors are known, the general solution of Eq. (22) is constructed using Eq. (13) and rearranged in the following form

$$x(t) = \Phi(t) \begin{Bmatrix} x_0 \\ \dot{x}_0 \end{Bmatrix}, \quad (28)$$

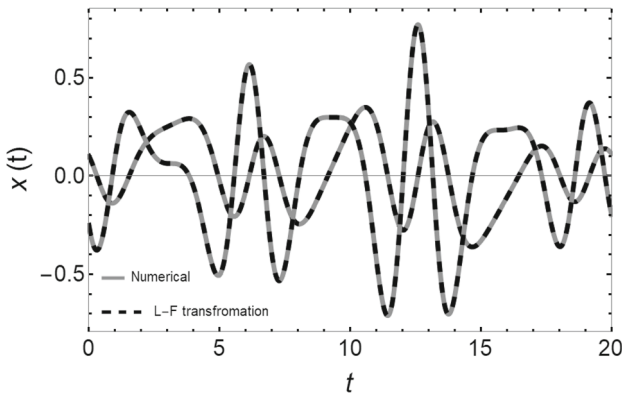
to obtain  $\Phi(t)$ . Using  $\Phi(T)$  and Eq. (8), the constant matrix  $\mathbf{R}$  is calculated and is given in Col. 6 of Table 1. Then,  $\Phi(t)$  and  $\mathbf{R}$  are substituted in Eq. (6) to compute the L–F transformation,  $\mathbf{Q}(t)$ . Application of L–F transformation reduces Eq. (22) to Eq. (7) which can be solved easily and the solution can be substituted in the transformation,  $\mathbf{x} = \mathbf{Q}(t)\mathbf{z}$  to get  $\mathbf{x}$ . Figure 2 compares the  $\mathbf{x}$  determined using L–F transformation with the  $\mathbf{x}$  obtained by the direct numerical integration of Eq. (22). It could be seen that both solutions match exactly demonstrating the correctness of  $\Phi(t)$ ,  $\mathbf{R}$  and  $\mathbf{Q}(t)$ .

Figure 3 shows the L–F transformation where  $Q_{uv}(t)$  represents the element corresponding to  $u^{th}$  row and  $v^{th}$  column of  $\mathbf{Q}(t)$ . The transformation is  $T$  periodic because the real parts of the Floquet multipliers have positive real part (see col. 5 of Table 1).



**Table 1** Different cases corresponding to the Mathieu equation

Case	$a$	$b$	$\lambda$	$\rho$	$R$
Col. 1	Col. 2	Col. 3	Col. 4	Col. 5	Col. 6
Stable	4	4	$\lambda_1 = +0.167285 i$ $\lambda_2 = -0.167285i$	$\rho_1 = 0.496631 + 0.867962i$ $\rho_2 = 0.496631 - 0.867962i$	$\begin{bmatrix} 0 & -0.0224983 \\ 1.24384 & 0 \end{bmatrix}$
Unstable	2.5	2.5	$\lambda_1 = 0.112754 + 0.5i$ $\lambda_2 = 0.112754 - 0.5i$	$\rho_1 = -2.03085$ $\rho_2 = -0.492404$	$\begin{bmatrix} 0 & -0.0989448 \\ -0.128491 & 0 \end{bmatrix}$
Critical	0.686720	2	$\lambda_1 = 0$ $\lambda_2 = 0$	$\rho_1 = +1$ $\rho_2 = +1$	$\begin{bmatrix} 0 & 0 \\ 4.37782 & 0 \end{bmatrix}$



**Fig. 2** Comparison of  $\mathbf{x}$  obtained using  $\mathbf{x} = \mathbf{Q}(t)\mathbf{z}$  with  $\mathbf{x}$  determined by numerical integration of Eq. (22) for the stable case

To develop the inverse of L–F transformation, the adjoint system of the damped Mathieu equation is defined as

$$\dot{\mathbf{x}} = \begin{bmatrix} 0 & (a + b \cos \omega t) \\ -1 & d \end{bmatrix} \mathbf{x}. \tag{29}$$

Using Eq. (11) in Eq. (29), the following two equations are obtained.

$$c_s^{11}(\lambda + is\omega) = ac_s^{12} + (b/2)(c_{s-1}^{12} + c_{s+1}^{12}), \tag{30a}$$

$$c_s^{12}(\lambda + is\omega) = -c_s^{11} + dc_s^{12}. \tag{30b}$$

They can be reduced to

$$[(\lambda + is\omega)^2 - d(\lambda + is\omega) + a]c_s^{12} + (b/2)(c_{s-1}^{12} + c_{s+1}^{12}) = 0, \tag{31}$$

and can be written in the matrix form as

$$\hat{\mathbf{K}}\hat{\mathbf{c}}^1 = \begin{bmatrix} k_{-N} & \frac{b}{2} & & & & & \\ & \frac{b}{2} & \ddots & & & & \\ & & \ddots & k_0 & \ddots & & \\ & & & & \ddots & & \\ & & & & & \frac{b}{2} & \\ & & & & & \frac{b}{2} & k_N \end{bmatrix} \begin{bmatrix} c_{-N}^{12} \\ \vdots \\ \vdots \\ \vdots \\ c_0^{12} \\ \vdots \\ \vdots \\ \vdots \\ c_N^{12} \end{bmatrix} = \begin{bmatrix} 0 \\ \vdots \\ \vdots \\ \vdots \\ 0 \\ \vdots \\ \vdots \\ \vdots \\ 0 \end{bmatrix}, \tag{32}$$

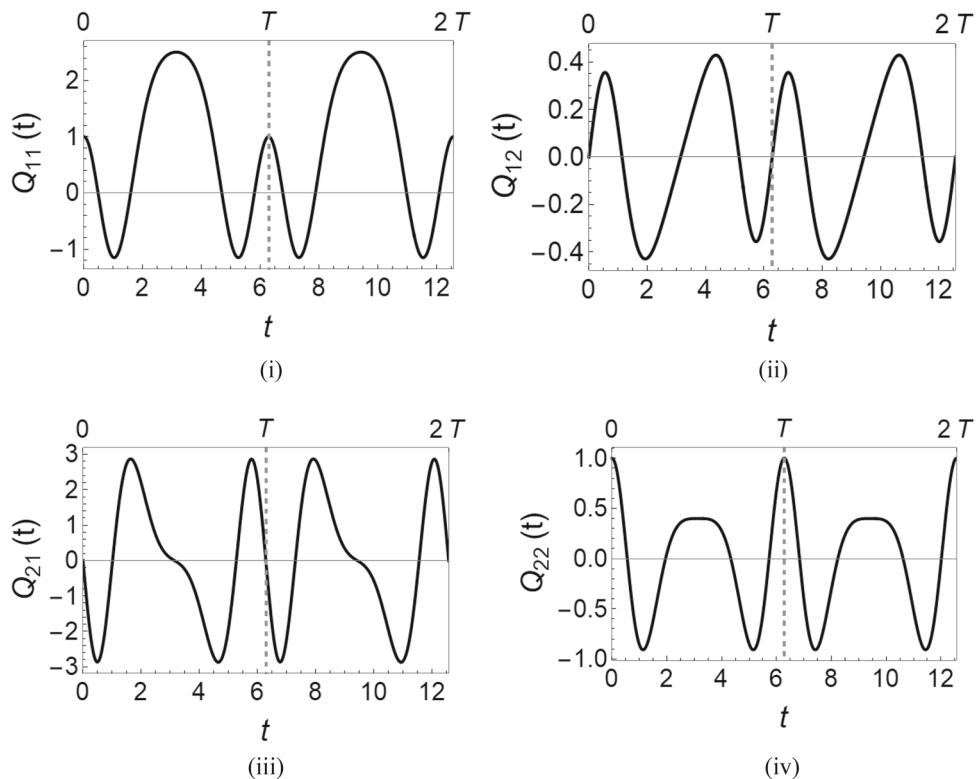
where  $k_s = [(\lambda + is\omega)^2 - d(\lambda + is\omega) + a]$ . With  $\omega = 1, d = 0, N = 10, a = 4$  and  $b = 4$  in Eq. (32), eigenvalues and eigenvectors are determined to construct the STM,  $\Psi(t)$  of the adjoint system, i.e., Eq. (29). Substitution of  $\Psi(t)$  in Eq. (21) yields the inverse of L–F transformation whose all four elements are shown in Fig. 4.  $Q_{uv}^{-1}(t)$  represents the element corresponding to  $u^{th}$  row and  $v^{th}$  column of  $\mathbf{Q}^{-1}(t)$ .

The solution of the Mathieu equation increases unboundedly for  $a = 2.5$  and  $b = 2.5$ . Similar to the stable case, the eigenvalues for the unstable case are distinct (see col. 4 Table 1). Therefore, the same process can be followed to construct  $\Phi(t), \mathbf{R}$  and  $\mathbf{Q}(t)$ .  $\mathbf{x}$  obtained using  $\mathbf{x} = \mathbf{Q}(t)\mathbf{z}$  matches well with the one determined by the direct numerical integration of Eq. (22) and is shown in Fig. 5. The transformation  $\mathbf{Q}(t)$  is  $2T$  periodic as the Floquet multipliers have negative real parts.  $\mathbf{Q}^{-1}(t)$  is obtained using Eqs. (32) and (21). For the sake of brevity figures showing  $\mathbf{Q}(t)$  and  $\mathbf{Q}^{-1}(t)$  are not included.

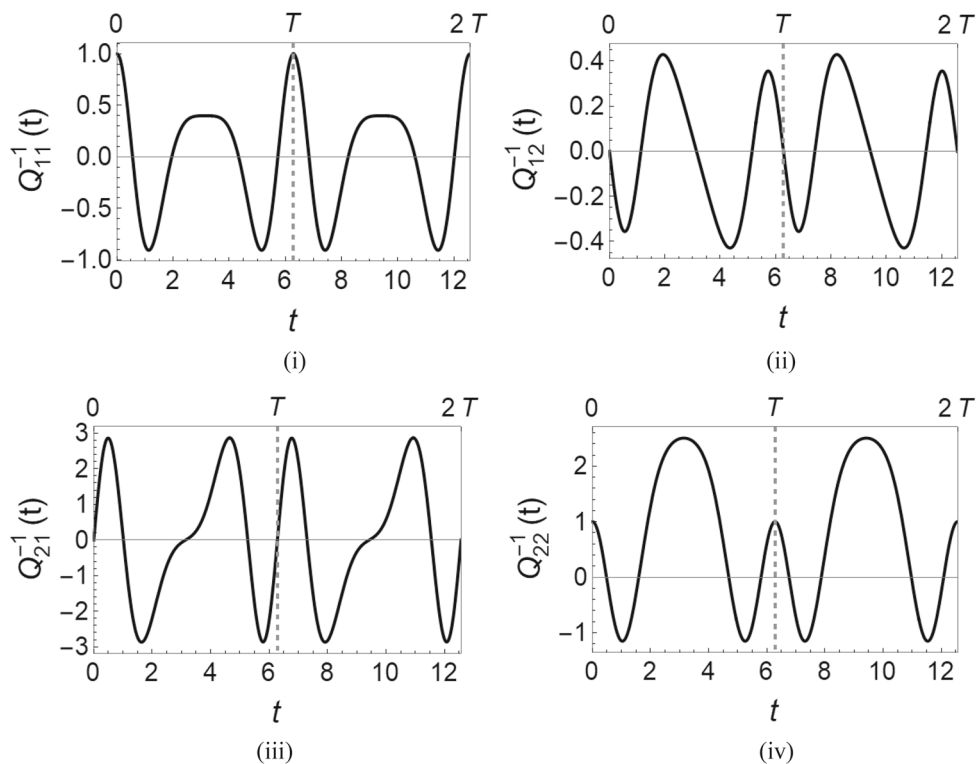
**4.1.2 L–F transformation and its inverse for a critical case**

The Mathieu equation is in a critical state for  $a = 0.686720$  and  $b = 2$ . Eigenvalues are 0 and 0 (not distinct) with algebraic multiplicity 2. Equation (23) yields only one linearly independent eigenvector,  $\mathbf{c}^1$  and the corresponding solution

**Fig. 3** L–F transformation for the stable case of the Mathieu Equation



**Fig. 4** The inverse of L–F transformation for the stable case of the Mathieu Equation



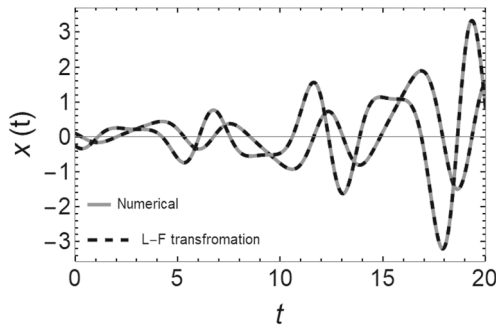


Fig. 5 Comparison of  $x$  obtained using  $x = Q(t)z$  with  $x$  determined by numerical integration of Eq. (22) for the unstable case

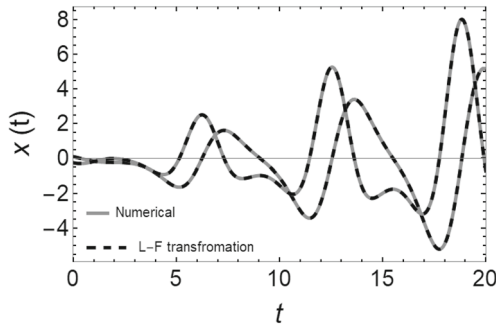


Fig. 6 Comparison of  $x$  obtained using  $x = Q(t)z$  with  $x$  determined by numerical integration of Eq. (22) for the critical case

is of the form of Eq. (11). Thus, the geometric multiplicity of the eigenvalue is 1. To determine the second linearly independent solution,

$$x = e^{\lambda t} \begin{Bmatrix} t p^{11}(t) + p^{21}(t) \\ t p^{12}(t) + p^{22}(t) \end{Bmatrix}, \tag{33}$$

is substituted in Eq. (22). Equating the coefficients of  $t$  and then  $e^{is\omega t}$  leads to Eq. (15a) whereas Eq. (15b) is obtained by matching the coefficients of  $t^0$  and then  $e^{is\omega t}$ . Equation (15a) is the same as Eq. (23) and has already been solved for  $c^1$  above.  $c^1$  obtained is then substituted in Eq. (15b) to calculate  $c^2$ . With  $c^1$  and  $c^2$  known, the general solution is constructed and then  $\Phi(t), R$  and  $Q(t)$  are determined. As shown in Fig. 6,  $x$  calculated using  $x = Q(t)z$  shows an excellent agreement with the solution obtained by numerically integrating Eq. (22). The similar process can be followed to compute the STM of the adjoint system and subsequently,  $Q^{-1}(t)$  can be calculated.

### 4.2 Double inverted pendulum

Consider a double inverted pendulum subjected to a time-periodic force as shown in Fig. 7. Linearized equations of motion around the equilibrium point  $(\phi_1, \phi_2) = (0, 0)$  can

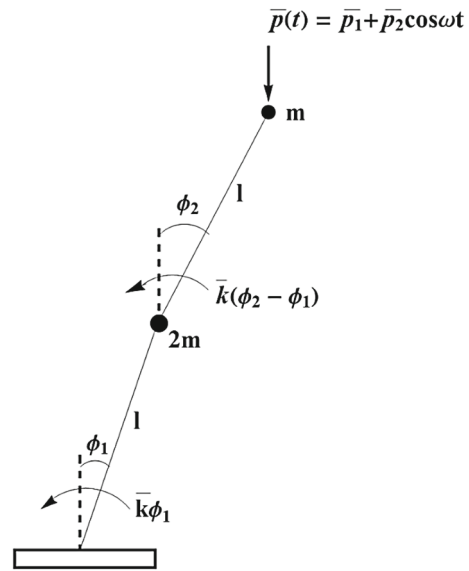


Fig. 7 A double inverted pendulum

be written in the state space form as

$$\begin{Bmatrix} \dot{x}_1 \\ \dot{x}_2 \\ \dot{x}_3 \\ \dot{x}_4 \end{Bmatrix} = \begin{bmatrix} 0 & 0 & 1 & 0 \\ 0 & 0 & 0 & 1 \\ (-3k + p(t))/2 & k - p(t)/2 & 0 & 0 \\ (5k - p(t))/2 & -2k + 1.5p(t) & 0 & 0 \end{bmatrix} \begin{Bmatrix} x_1 \\ x_2 \\ x_3 \\ x_4 \end{Bmatrix}, \tag{34}$$

where  $k = \bar{k}/ml^2, p(t) = \bar{p}(t)/ml$  and  $\bar{p}(t) = \bar{p}_1 + \bar{p}_2 \cos \omega t$ . Here,  $m$  = mass of the link,  $l$  = length of the link,  $\bar{k}$  = stiffness parameter,  $\bar{p}_1$  = static load,  $\bar{p}_2$  = amplitude of the parametric excitation term,  $\phi_1$  and  $\phi_2$  are the displacement angles and the state vector is defined as  $\{x_1, x_2, x_3, x_4\}^T = \{\phi_1, \phi_2, \phi_1', \phi_2'\}^T$ .

Substitution of Eq. (11) with  $n = 4$  in Eq. (34) and equating the coefficients of  $e^{is\omega t}$  yields

$$c_s^{11}(\lambda + is\omega) = c_s^{13}, \tag{35a}$$

$$c_s^{12}(\lambda + is\omega) = c_s^{14}, \tag{35b}$$

$$c_s^{13}(\lambda + is\omega) = A_s + B_{s-1} + B_{s+1}, \tag{35c}$$

$$c_s^{14}(\lambda + is\omega) = C_s + D_{s-1} + D_{s+1}, \tag{35d}$$

where  $A_s = [c_s^{11}(-3k + p_1)/2] + [(k - p_1/2)c_s^{12}]$ ,  $B_s = [(c_s^{11} - c_s^{12})p_2/4]$ ,  $C_s = [c_s^{11}(5k - p_1)/2] + [(-2k + 3p_1/2)c_s^{12}]$  and  $D_s = [(3c_s^{12} - c_s^{11})p_2/4]$ . Substitution of  $c_s^{13}$  from Eq. (35a) and  $c_s^{14}$  from Eq. (35b) in Eqs. (35c) and (35d), respectively, leads to

$$c_s^{11}(\lambda + is\omega)^2 = A_s + B_{s-1} + B_{s+1}, \tag{36a}$$



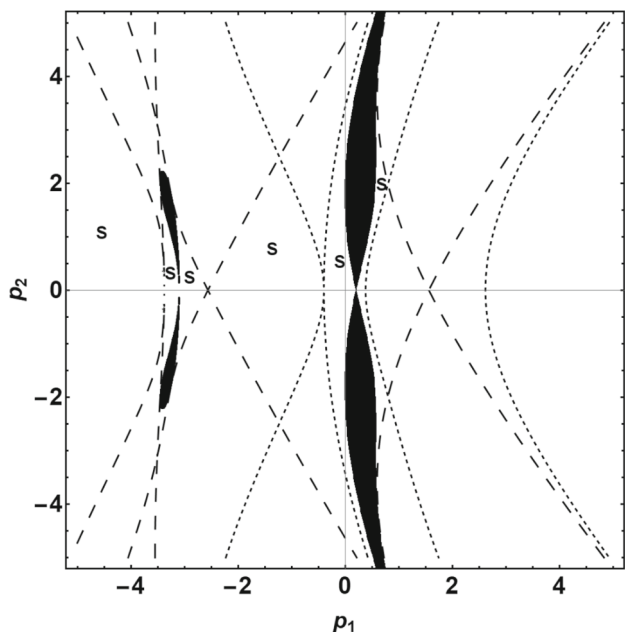


**Fig. 8** Stability diagram of the double inverted pendulum. Large dashes:  $2T$  periodic boundaries, Small dashes:  $T$  periodic boundaries, Solid black: Unstable regions due to combination resonances and S denotes stable regions

$$c_s^{12}(\lambda + is\omega)^2 = C_s + D_{s-1} + D_{s+1}, \tag{36b}$$

which can be expressed in matrix form  $\overline{\mathbf{K}} \overline{\mathbf{c}}^1 = \mathbf{0}$  with  $\overline{\mathbf{c}}^1 = \{c_{-N}^{11} \dots c_N^{11} \ c_{-N}^{12} \dots c_N^{12}\}^T$ .

Equation (34) can become unstable due to parametric and combination resonances. With  $k = 1$  and  $\omega = 2$ ,  $\text{Det}[\overline{\mathbf{K}}]$  is set to zero to obtain the polynomial expressions for the stability boundaries of  $T$  and  $2T$  periodic unstable regions by substituting  $\lambda$  as 0 and  $i\pi/T$ , respectively. Unstable regions due to combination resonances can be only found by calculating exponents at sample points. They cannot overlap  $T$  and  $2T$  periodic unstable regions as four eigenvalues are required for combination resonances. Figure 8 shows the stability diagram of Eq. (34) in  $p_1 \sim p_2$  plane for  $N = 10$  and is in good agreement with the numerically computed diagram (not shown).

#### 4.2.1 L–F transformation and its inverse for a critical case

Equation (34) is in a critical state for  $(p_1, p_2) = (0.570366, 2)$ . The point lies on the boundary of the combination resonance region that is in the upper right half plane of the stability diagram, and the corresponding eigenvalues are  $0.455552i, 0.455552i, -0.455552i$  and  $-0.455552i$ . Eigenvalues  $0.455552i$  and  $-0.455552i$  are repeated twice (algebraic multiplicity 2) and each of them only yields one linearly independent eigenvector (geometric multiplicity 1)

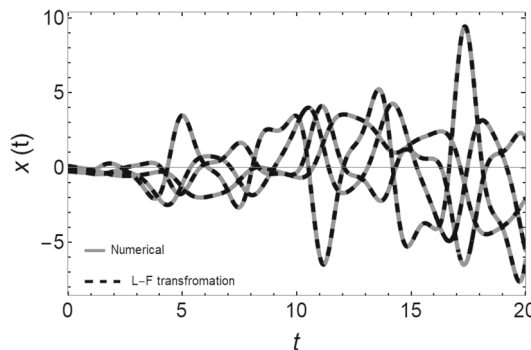


**Fig. 9** Comparison of  $\mathbf{x}$  obtained using  $\mathbf{x} = \mathbf{Q}(t)\mathbf{z}$  with  $\mathbf{x}$  determined by numerical integration of Eq. (34) for the critical case

which can be obtained using the matrix form of Eq. (36). To construct the general solution, one more linearly independent eigenvector is needed for both  $0.455552i$  and  $-0.455552i$  and thus, the following form of solution must be assumed and substituted in Eq. (34) for each eigenvalue.

$$\mathbf{x} = e^{\lambda t} \begin{Bmatrix} tp^{11}(t) + p^{21}(t) \\ tp^{12}(t) + p^{22}(t) \\ tp^{13}(t) + p^{23}(t) \\ tp^{14}(t) + p^{24}(t) \end{Bmatrix}. \tag{37}$$

As observed in Sec 4.1.2, equating the coefficients of  $t$  and then  $e^{is\omega t}$  yields Eq. (35), which has been solved before for  $c_s^{11}, c_s^{12}, c_s^{13}$  and  $c_s^{14}$  to get the solution of the form of Eq. (11). Comparing the coefficients of  $t^0$  and then  $e^{is\omega t}$  leads to

$$c_s^{11} + c_s^{21}(\lambda + is\omega) = c_s^{23}, \tag{38a}$$

$$c_s^{12} + c_s^{22}(\lambda + is\omega) = c_s^{24}, \tag{38b}$$

$$c_s^{13} + c_s^{23}(\lambda + is\omega) = \overline{A}_s + \overline{B}_{s-1} + \overline{B}_{s+1}, \tag{38c}$$

$$c_s^{14} + c_s^{24}(\lambda + is\omega) = \overline{C}_s + \overline{D}_{s-1} + \overline{D}_{s+1}, \tag{38d}$$

where  $\overline{A}_s = [c_s^{21}(-3k + p_1)/2] + [(k - p_1/2)c_s^{22}]$ ,  $\overline{B}_s = [(c_s^{21} - c_s^{22})p_2/4]$ ,  $\overline{C}_s = [c_s^{21}(5k - p_1)/2] + [(-2k + 3p_1/2)c_s^{22}]$  and  $\overline{D}_s = [(3c_s^{22} - c_s^{21})p_2/4]$ .  $c_s^{23}$  from Eq. (38a) and  $c_s^{24}$  from Eq. (38b) are substituted in Eqs. (38c) and (38d) which are then solved to determine the second independent eigenvector for each eigenvalue ( $0.455552i$  and  $-0.455552i$ ). Subsequently, the STM and the L–F transformation can be constructed. Once again, an excellent agreement between  $\mathbf{x}$  computed using  $\mathbf{x} = \mathbf{Q}(t)\mathbf{z}$  and  $\mathbf{x}$  obtained by direct numerical integration of Eq. (34) is observed and shown in Fig. 9. The STM for the adjoint system to Eq. (34) can be determined following a similar process and  $\mathbf{Q}^{-1}(t)$  can be computed. Figure 10 shows the elements

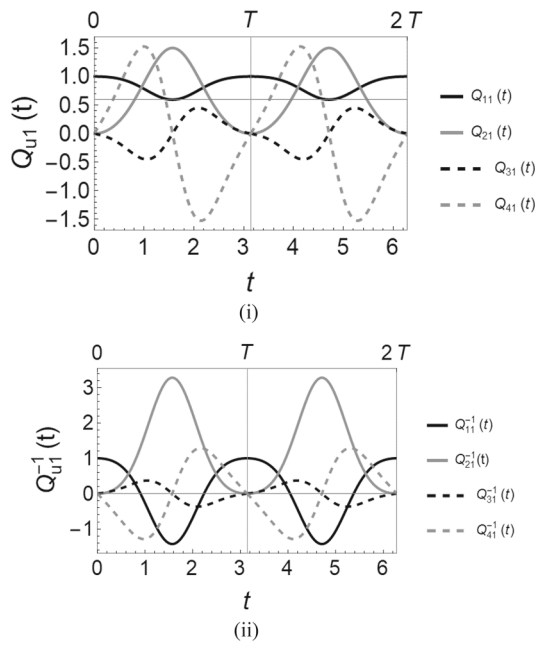


**Fig. 10** The elements corresponding to the first column of L–F transformation and its inverse for the critical case

corresponding to the first column L–F transformation and its inverse.

### 5 Application: bifurcation study

The present section demonstrates one of the applications of L–F transformation by performing the bifurcation analysis of a nonlinear time-periodic system using the center manifold reduction theory [20]. As an example, a damped Mathieu equation with cubic nonlinearity is considered.

$$\begin{Bmatrix} \dot{x}_1 \\ \dot{x}_2 \end{Bmatrix} = \begin{bmatrix} 0 & 1 \\ -(a + b \cos \omega t) & -d \end{bmatrix} \begin{Bmatrix} x_1 \\ x_2 \end{Bmatrix} + \begin{Bmatrix} 0 \\ -\varepsilon x_1^3 \end{Bmatrix}, \quad (39)$$

For  $a = 3.9177873446$ ,  $b = 4$ ,  $d = 0.31623$  and  $\omega = 2$ , Floquet multipliers are found to be 0.37029109302 and 0.99999999991, implying that the system undergoes fold bifurcation and gives rise to a  $T$  periodic solution. Following the process given in Sect. 3, first  $\Phi(t), \mathbf{R}, \mathbf{Q}(t)$  and  $\mathbf{Q}^{-1}(t)$  are computed and then using the transformation  $\mathbf{x} = \mathbf{Q}(t)\mathbf{z}$ , Eq. (39) is reduced to

$$\begin{Bmatrix} \dot{z}_1 \\ \dot{z}_2 \end{Bmatrix} = \underbrace{\begin{bmatrix} -0.155676 & 0.0154273 \\ 1.62014 & -0.160554 \end{bmatrix}}_{\mathbf{R}} \begin{Bmatrix} z_1 \\ z_2 \end{Bmatrix} + \mathbf{Q}^{-1}(t) \begin{Bmatrix} 0 \\ -\varepsilon (Q_{11}z_1 + Q_{12}z_2)^3 \end{Bmatrix}. \quad (40)$$

An application of modal transformation,  $\mathbf{z} = \mathbf{M}\mathbf{y}$  to the above system yields,

$$\begin{Bmatrix} \dot{y}_1 \\ \dot{y}_2 \end{Bmatrix} = \begin{bmatrix} -0.31623 & 0 \\ 0 & 0 \end{bmatrix} \begin{Bmatrix} y_1 \\ y_2 \end{Bmatrix} + \mathbf{M}^{-1}\mathbf{Q}^{-1}(t) \begin{Bmatrix} 0 \\ -\varepsilon (Q_{11} (M_{11}y_1 + M_{12}y_2) + Q_{12} (M_{21}y_1 + M_{22}y_2))^3 \end{Bmatrix}. \quad (41)$$

Due to the periodic nature of  $\mathbf{Q}(t)$  and  $\mathbf{Q}^{-1}(t)$ , the coefficients of the nonlinear part of the above equation can be expanded using the Fourier expansion. Thus, Eq. (41) can be rewritten as

$$\begin{Bmatrix} \dot{y}_1 \\ \dot{y}_2 \end{Bmatrix} = \begin{bmatrix} -0.31623 & 0 \\ 0 & 0 \end{bmatrix} \begin{Bmatrix} y_1 \\ y_2 \end{Bmatrix} + \begin{Bmatrix} f_{11}(t)y_1^3 + f_{12}(t)y_1^2y_2 + f_{13}(t)y_1y_2^2 + f_{14}(t)y_2^3 \\ f_{21}(t)y_1^3 + f_{22}(t)y_1^2y_2 + f_{23}(t)y_1y_2^2 + f_{24}(t)y_2^3 \end{Bmatrix}, \quad (42)$$

where  $f_{ij}(t) = f_{ij}(t + T)$ ;  $i = 1, 2$  and  $j = 1, \dots, 4$ . One of the eigenvalues is critical ( $\lambda_2 = 0$ ) and thus, the center manifold theorem [20] can be applied to reduce the dimension of Eq. (42) to one.

According to the theorem, the center manifold relation has the form

$$y_1 = h(t)y_2^3, \quad (43)$$

where  $h(t)$  is a periodic coefficient with period  $T$ . Substitution of Eq. (43) into  $\dot{y}_1$  equation of Eq. (42) leads to

$$\frac{dh(t)}{dt} + 0.31623h(t) = f_{14}(t). \quad (44)$$

$h(t)$  can be determined by solving the above differential equation. Substituting the finite Fourier expansion of the form

$$h(t) = \frac{a_0}{2} + \sum_{\bar{n}=1}^{N_1} a_{\bar{n}}\text{Cos } \bar{n}\omega t + b_{\bar{n}}\text{Sin } \bar{n}\omega t, \quad (45)$$

in Eq. (44) and then equating like terms on both sides of the equation yields a set of algebraic equations in terms of unknown constants  $a_0, a_{\bar{n}}$  and  $b_{\bar{n}}$  of the center manifold relation. Once constants are known, substitution of relation (43) in Eq. (42) decouples the critical state from the stable one and the bifurcation analysis can be performed by investigating the one-dimension system in the center manifold. Keeping only the cubic terms leads to

$$\dot{y}_2 = f_{24}(t)y_2^3. \quad (46)$$

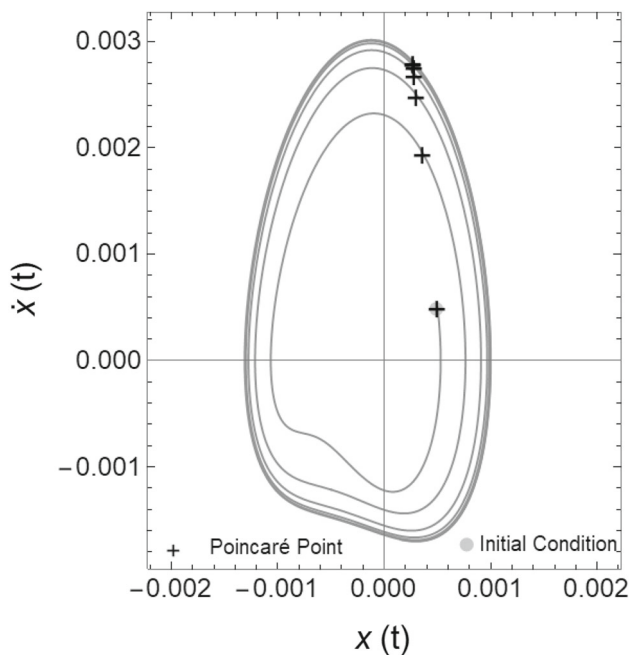


**Fig. 11** Phase plane plot for the nonlinear Mathieu equation given by Eq. (39)

According to the center manifold theory, the reduced equation, Eq. (46) is dynamically equivalent to the original system, Eq. (39). Therefore, if the above equation is asymptotically stable (unstable), the original system is also asymptotically stable (unstable). Since the coefficient of the right-hand side of Eq. (46) is periodic, the constant term,  $(a_0/2)$  in the Fourier series of  $f_{24}(t)$  determines the stability. If  $(a_0/2)$  is negative, the periodic solution is asymptotically stable, otherwise unstable. It is found that in Eq. (46),  $(a_0/2) = 0.0109$  and therefore, the resulting  $T$  periodic solution is unstable. Figure 11 shows the phase plane plot and the Poincaré map of Eq. (39). It can be observed that the Poincaré points corresponding to the  $T$  periodic orbit are drifting away, representing the unstable behavior of the solution.

### 6 Discussion and conclusions

The paper presents a simple approach for the computation of Lyapunov–Floquet (L–F) transformations. These transformations replace a set of ordinary differential equations with time-periodic coefficients (so-called time-periodic systems) with dynamically equivalent systems whose linear parts are time-invariant. As a result, the reduced equations can be analyzed using techniques used for time-invariant systems.

In the proposed approach, the solution of a time-periodic system,  $\dot{\mathbf{x}} = \mathbf{A}(t)\mathbf{x}$ ;  $\mathbf{A}(t + T) = \mathbf{A}(t)$  is assumed as  $\mathbf{x} = e^{\lambda t} \mathbf{p}^1(t)$  where  $\lambda$  is the characteristic exponent, and  $\mathbf{p}^1(t)$  is a

periodic vector function with principal period  $T$ . With  $\mathbf{p}^1(t)$  expressed in the complex form of finite Fourier series, the substitution of the assumed solution in the time-periodic system leads to an eigenvalue problem  $\mathbf{K}(\bullet)\mathbf{c}^1 = \mathbf{0}$  where  $\mathbf{K}(\bullet)$  consist of system parameters,  $\lambda$  and the parametric excitation frequency and  $\mathbf{c}^1$  is a vector containing the unknown coefficients of the Fourier series of  $\mathbf{p}^1(t)$ . Eigenvalues can be found by setting  $\text{Det}[\mathbf{K}(\bullet)] = 0$  and their number depend upon the dimension of the system,  $\dot{\mathbf{x}} = \mathbf{A}(t)\mathbf{x}$  and the number of terms in the Fourier series of  $\mathbf{p}^1(t)$ . The number of eigenvalues should be same as the dimension of the time-periodic system and can be determined using the constraint  $-\pi/T < \text{Im}[\lambda] \leq \pi/T$ . Once eigenvalues are known, corresponding eigenvectors,  $\mathbf{c}^1$  can be determined from  $\mathbf{K}(\bullet)\mathbf{c}^1 = \mathbf{0}$  and the general solution and subsequently, the state transition matrix,  $\Phi(t)$  can be constructed. It must be noted that all linearly independent solutions forming the general solution have the form  $\mathbf{x} = e^{\lambda t} \mathbf{p}^1(t)$  only when the eigenvalues are distinct. If eigenvalue  $\lambda$  has algebraic multiplicity  $\Gamma$ , geometric multiplicity  $\Lambda$  and  $\Gamma > \Lambda$ , then, there are  $\Lambda$  linearly independent solutions of the form  $\mathbf{x} = e^{\lambda t} \mathbf{p}^1(t)$ . To get the remaining  $(\Gamma - \Lambda)$  linearly independent solutions,  $\mathbf{x} = e^{\lambda t} [t\mathbf{p}^1(t) + \mathbf{p}^2(t)]$  must be assumed and substituted in the system to yield  $\mathbf{K}(\bullet)\mathbf{c}^1 = \mathbf{0}$  and  $\mathbf{K}(\bullet)\mathbf{c}^2 = \mathbf{c}^1$ . With  $\mathbf{c}^1$  already known,  $\mathbf{c}^2$  can be obtained from the second equation and subsequently, an additional  $\Upsilon$  linearly independent solutions of the form  $\mathbf{x} = e^{\lambda t} [t\mathbf{p}^1(t) + \mathbf{p}^2(t)]$  can be generated. This process continues until there are  $\Gamma$  linearly independent solutions corresponding to eigenvalue,  $\lambda$ . After determining the solutions for all eigenvalues, the general solution can be found and subsequently rearranged in the form of Eq. (4) to obtain  $\Phi(t)$ . Then, Lyapunov–Floquet theorem [9] can be applied to compute time-invariant matrix  $\mathbf{C}$ (or  $\mathbf{R}$ ) and L–F transformations  $\mathbf{L}(t)$  (or  $\mathbf{Q}(t)$ ). The inverse of L–F transformations required for the analysis of nonlinear time-periodic systems can be determined by defining the adjoint system to  $\dot{\mathbf{x}} = \mathbf{A}(t)\mathbf{x}$ .

The proposed approach is utilized to investigate Mathieu equation and a double inverted pendulum subjected to a time-periodic force. Stability diagrams are plotted for large values of system parameters and are found to be in excellent agreement with the numerically obtained diagrams. These diagrams were constructed to determine the values of system parameters for stable, unstable and critical cases. In the case of Mathieu equation, L–F transformations and their inverses are generated for stable, unstable and critical cases whereas, for the double inverted pendulum, L–F transformation and its inverse are constructed only for the critical case. The solutions obtained through L–F transformations matched the numerically obtained solutions for both time-periodic systems. A bifurcation study is also performed for a nonlinear Mathieu equation using L–F transformation and center manifold theory to show the efficacy of L–F transformations. The

behavior predicted by the reduced scalar equation matched with that of the original system.

In summary, a simple technique for the computation of L–F transformations is presented in the paper. The approach is applicable to general time-periodic systems and through the application of L–F transformations, techniques used for time-invariant systems can be applied to general time-periodic systems.

**Acknowledgements** None.

**Author's contribution** Conceptualization, investigation, methodology and writing original and final drafts.

**Funding** The author declares that no funds, grants, or other support were received during the preparation of this manuscript.

**Data availability** No data were generated in this manuscript.

## Declarations

**Competing interests** The authors have no relevant financial or non-financial interests to disclose.

## References

1. Mathieu É (1868) Mémoire sur le mouvement vibratoire d'une membrane de forme elliptique. *J Math Pures Appl* 13:137–203
2. Floquet MG (1883) Sur les équations différentielles linéaires à coefficients périodiques. *Ann Sci l'École Normale Supérieure* 12(2):47–88. <https://doi.org/10.24033/asens.220>
3. Grimshaw R (1990) *Nonlinear ordinary differential equations*. Blackwell Scientific Publications, Hoboken
4. Friedmann P, Hammond CE, Woo TH (1977) Efficient numerical treatment of periodic systems with application to stability problems. *Int J Numer Methods Eng* 11(7):1117–1136. <https://doi.org/10.1002/nme.1620110708>
5. Nayfeh AH, Mook DT (1979) *Nonlinear oscillations*. Wiley, New York
6. Sanders JA, Verhulst F (1985) *Averaging methods in nonlinear dynamical systems*. Springer, New York
7. Sinha SC, Butcher EA (1997) Symbolic computation of fundamental solution matrices for time periodic dynamical systems. *J Sound Vib* 206(1):61–85. <https://doi.org/10.1006/jsvi.1997.1079>
8. Kirkland GW, Sinha SC (2016) Symbolic computation of quantities associated with time-periodic dynamical systems. *ASME J Comput Nonlin Dyn* 11(4):041022. <https://doi.org/10.1115/1.4033382>
9. Yakubovich VA, Starzhinski VM (1975) *Linear differential equations with periodic coefficients-part I*. Wiley, New York
10. Pandiyan R, Sinha SC (1995) Analysis of time-periodic nonlinear dynamical systems undergoing bifurcations. *Nonlinear Dyn* 8(1):21–43. <https://doi.org/10.1007/BF00045005>
11. Dávid A, Sinha SC (2000) Versal deformation and local bifurcation analysis of time-periodic nonlinear systems. *Nonlinear Dyn* 1(4):317–336. <https://doi.org/10.1023/A:1008330023291>
12. Deshmukh VS, Sinha SC (2004) Control of dynamic systems with time-periodic coefficients via the Lyapunov–Floquet transformation and backstepping technique. *J Vib Control* 10(10):1517–1533. <https://doi.org/10.1177/1077546304042064>
13. Zhang Y, Sinha SC (2009) Observer design for nonlinear systems with time-periodic coefficients via normal form theory. *ASME J Comput Nonlin Dyn* 4(3):031001. <https://doi.org/10.1115/1.3124093>
14. Sinha SC, Pandiyan R (1994) Analysis of quasilinear dynamical systems with periodic coefficients via Liapunov–Floquet transformation. *Int J Nonlinear Mech* 29(5):687–702. [https://doi.org/10.1016/0020-7462\(94\)90065-5](https://doi.org/10.1016/0020-7462(94)90065-5)
15. Lukes DL (1982) *Differential equations: classical to controlled*. Academic Press, New York
16. Sinha SC, Wu DH (1991) An efficient computational scheme for the analysis of periodic systems. *J Sound Vib* 151(1):91–117. [https://doi.org/10.1016/0022-460X\(91\)90654-3](https://doi.org/10.1016/0022-460X(91)90654-3)
17. Pandiyan R, Bibb JS, Sinha SC (1996) Liapunov–Floquet transformation: computation and application to periodic systems. *J Vib Acoust* 118(2):209–219. <https://doi.org/10.1115/1.2889651>
18. Butcher EA, Sari Ma'en S, Carlson T (2009) Magnus' expansion for time-periodic systems: parameter-dependent approximation. *Commun Nonlinear Sci Numer Simul* 14(12):4226–4245. <https://doi.org/10.1016/j.cnsns.2009.02.030>
19. Hill GW (1886) On the part of the motion of the lunar perigee which is a function of the mean motions of the sun and moon. *Acta Math* 8:1–36. <https://doi.org/10.1007/BF02417081>
20. Malkin IG (1962) Some basic theorems of the theory of stability of motion in critical cases. In: *Stability and dynamic systems translations*, American Mathematical Society Series 1, vol 5, pp 242–290

Springer Nature or its licensor (e.g. a society or other partner) holds exclusive rights to this article under a publishing agreement with the author(s) or other rightsholder(s); author self-archiving of the accepted manuscript version of this article is solely governed by the terms of such publishing agreement and applicable law.